

# Colouring monohedral tilings: defects and grain boundaries

Giedrius Alkauskas

Institute of Computer Science, Vilnius University, Naugarduko 24, Vilnius, LT-03225, Lithuania. Email: `giedrius.alkauskas@mif.vu.lt`.

arXiv:2301.10975v3 [math.CO] 14 Sep 2024

## 1 Aperiodicity

This paper describes a novel phenomenon in the theory of tilings – a *grain boundary* (1D defect in a 2D material) forced by a finite patch. We discuss the *structure*, and (in lesser extent) *the growth* of the obtained quasicrystal (more aptly, a *polycrystal*).

In the theory of tilings, the pivotal and long awaited-for recent achievement is the discovery of a polygon (one piece, or the *einstein*) which tiles the whole plane, but only non-periodically [8, 10]. A nice introduction to the subject appeared in the *Intelligencer* as a homage to the legacy of John Conway [6]. Another paper in this journal [12] by Socolar and Taylor describes nicely many aspects in the field: what is a tile; what is a tiling; what is considered to be non-periodic; what are possible matching rules. There is no need to list all the cornerstones of this fascinating story here, specialists can do it better. The reader of this paper will benefit greatly (as did the author) in deeper acquaintance with the works cited. The term *forced* means that the initial data determines the final object uniquely.

In this note we show a forced full tiling, which leads to something non-periodic, but still surprisingly simple and well-organized. The final object may be thought as being formed by parts of different crystals along with *grain boundaries*; these are interfaces between any two. All results fit into a much broader framework of 2-periodic discrete planar graphs and problem of *unique colorability*, the approach most convenient to work with. However, in Section 7 we will demonstrate that the whole setting has an interpretation which perfectly fits in the framework described by Taylor and Socolar [12] (p. 20-21), and also by Ballier, Durand and Jeandel ([2], Section 2).

In our case we have a single **simply connected**

tile. Concerning the matching rules, **only rotations** are allowed, moreover, **a finite number** of them; **colors required**; **only adjacent** tiles must match (having a common vertex is also considered to be adjacent). The implication is then as follows: there exist periodic tilings, but some seeds force non-periodic, though well-structured ones.

The connoisseur in the field, if only given these these vague descriptions, would raise an eyebrow. Indeed, consider the Taylor-Socolar tile [12, 13]. It is the first example of an *einstein*, with a slight caveat of being non-connected. To form a tiling, one needs its mirror copy, too. We emphasize one important feature: there exists a certain 3 tile seed which forces the full tiling ([12], p. 26-27). This unique object has a complicated combinatorial structure with relation to regular paperfolding sequences. It is important to note that the seed itself does not violate matching rules. This appears to be in contrast with a *decapod defect* in the Penrose tile setting ([11], p. 240). The latter forces a tiling, too, but the interior of a decapod cannot be filled with Penrose tiles without violating the rules.

In this light, the non-periodic and non-defective structure we obtain is much simpler. What is the trickery here? It is simple: we use a cubic tile where 4 pairs of opposite vertices are painted in 4 different colors. However, under the property “only rotations are allowed” we implicitly declare 3D rotations allowable, too. All permutations of main diagonals form a symmetry group of the cube, and all 24 rotations are needed.

This 3D construction seems to be astray of the main directions of research in the field. However, in order to realize matching rules for the connected Taylor-Socolar tile, one can produce a 3D version of it [12]. As a result, these tiles fill up a thickened plane  $\mathbb{R}^2 \times [0, 1]$ . Another example: the same paper

cite the (unpublished) construction of D. Fletcher in which an aperiodic tiling is obtained from 21 orientation of a single cubic tile and an atlas of allowable configurations. Finally, since part of the motivation in the area of non-periodic tilings comes from physics, we believe that an euclido-geometric model of the same tiling proposed later in Section 7 is a serious candidate to be realizable in the physical world.

*Dedication.* This paper is dedicated to the memory of Audrius Alkauskas (1978-2023). A physicist, an expert in the field of defects in semiconductors [1]. A musician and a writer. My dear twin brother.

## 2 The setting

Consider (not necessarily edge-to-edge) tessellation of the plane with a single tile (these are called *monohedral*), which at the same time is periodic [7]. We say that two tiles are *adjacent* if they share a common point.<sup>1</sup> Given  $N$  colors. We say that a tiling is  $N$ -colorable, if each tile can be assigned one of  $N$  colors in such a way that no two adjacent tiles share the same color.

The tiling is said to be *uniquely  $N$ -colorable*, if such a coloring can be performed (up to permutation of colors) in the unique way. For example, Picture 1 shows pentagonal tiling of type 3 (discovered by K. Reinhardt) and its unique 3-coloring.

If one wonders whether a unique  $N$ -coloring can be non-periodic, then the answer is, certainly, “No”. Indeed, let us color the whole plane. Let  $(\mathbf{a}, \mathbf{b})$  be any primitive pair of vectors of periodicity. Shift the tiling with respect  $\mathbf{a}$ . The new tiling, by definition, is obtained from the old one by a permutation of colors. This shows that the colored tiling is periodic with basis vectors being  $k \cdot \mathbf{a}$  and  $l \cdot \mathbf{b}$  for certain  $k, l \in \mathbb{N}$ . Moreover,  $k, l$  divide  $g(N)$ , where  $g(N)$  is Landau’s function (sequence A000793 in the On-Line Encyclopedia of Integer Sequences), the largest order of an element in the symmetric group  $S_N$ , which starts as follows:

$$1, 2, 3, 4, 6, 6, 12, 15, 20, 30, 30, 60, 60, 84, 105.$$

Thus, picture 2 shows another uniquely 3-colorable pentagonal tiling of type 2 (also discovered by Reinhardt), where the corresponding vectors are  $3 \cdot \mathbf{a}$

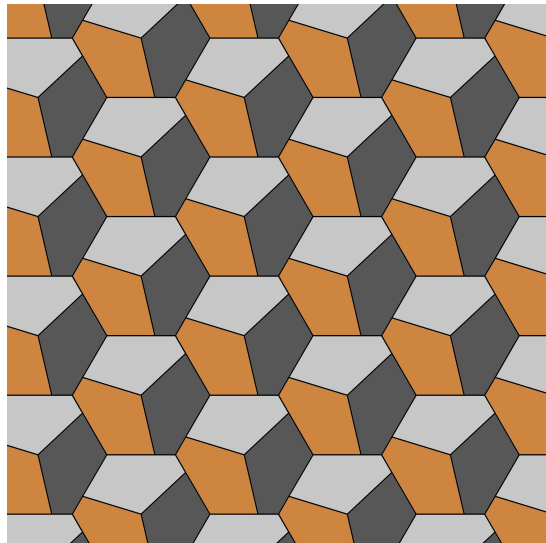


Fig. 1 Pentagonal tiling of type 3 (isohedral)

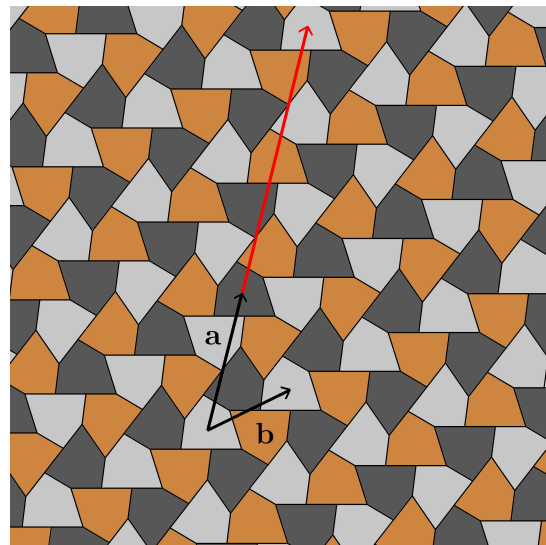


Fig. 2 Pentagonal tiling of type 2 (isohedral)

and  $\mathbf{b}$ .<sup>2</sup> The same phenomenon occurs for type 12 tiling (discovered by M. Rice, Figure 3). However, the latter is 2-isohedral (automorphism group of the tiling has 2 transitivity classes). As described in [4], these specific examples confirm a general rule: without a seed tile, there is no possibility of forcing an aperiodic tiling through local assembly rules.

<sup>1</sup>Usually tiles sharing a point are called *neighbouring*, to distinguish from those sharing a section of the border (*adjacent*). Yet, the precise definition has only an impact on formation of an adjacency graph. When that done, the term *adjacent* takes its standard meaning used in graph theory.

<sup>2</sup>As is clear from Figure 2, for a primitive pair  $(\mathbf{a}, \mathbf{a} - \mathbf{b})$ , the corresponding vectors would be  $(3\mathbf{a}, 3\mathbf{a} - 3\mathbf{b})$ . Therefore a pair  $(k, l)$  is also not uniquely defined. Finding a maximum value for  $k \cdot l$  (denote this by  $t(N)$ ) over all uniquely  $N$ -colorable tilings (more generally,  $N$ -colorable 2-periodic planar graphs) is a separate interesting problem. We know that  $t(N) \leq g^2(N)$ , which is an equality for  $N = 3$ .

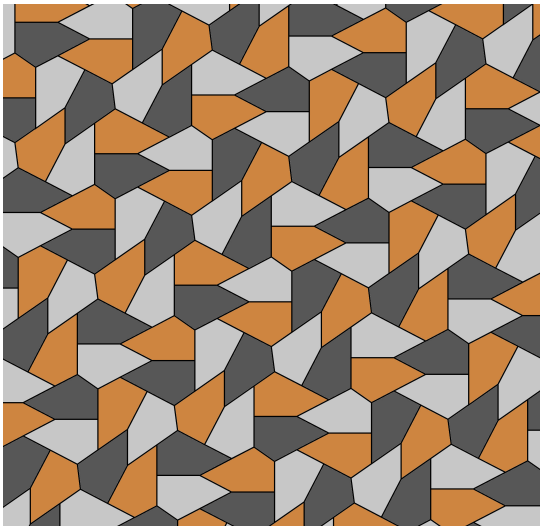


Fig. 3 Pentagonal tiling of type 12 (2-isohedral)

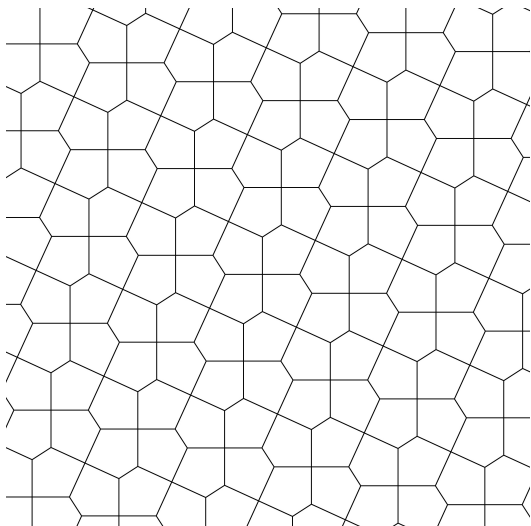


Fig. 4 Pentagonal type 4 tiling

### 3 A generic seed

Minding the unique colorability property, how one could obtain a uniquely defined aperiodic structure? An analogy with Turing machines and tilings which emulates them (see [8]) indicates the possible solution. Indeed, Turing machine is defined by a finite number of states, a finite number of symbols, and a transition function. It starts working when being fed some finite data tape. If we imagine that the unique colorability problem corresponds to an empty (all 0's) tape, then the answer is self-evident.

Given  $N$  colors. Start from a finite number of colored tiles. Call this *a seed*. The only requirement is that this collection does not conflict with the adjacency rule. If the remaining tiles can be colored in exactly  $r \in \mathbb{N}$  ways, the initial collection is called *a*

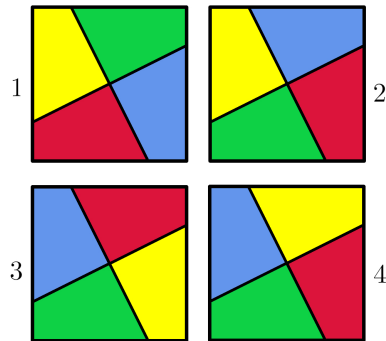


Fig. 5 4 (out of 24) tiling states

*decent seed* of order  $r$ . If the coloring is unique, seed is called *perfect*. This is a decent seed of order 1. It produces the colored tiling, which we also call *perfect*.

Obviously, if one start from any finite subset of colored tiles in, say, type 2 pentagonal tiling, then either the seed is contradictory, or Figure 2 is obtained, with (possibly) colors permuted.

Consider instead a famous Cairo pentagonal tiling (Figure 4). For convenience, we will work with topologically equivalent "split-chessboard" domino tiling (Figure 6), which we label *D-Cairo*. Assume that vertices where 4 tiles meet form an integer lattice  $\mathbb{Z}^2$ . Fix  $N = 4$  colors: **Red**, **Green**, **Blue**, and **Yellow**.

To demonstrate that the graph colorability problem in consideration is a special case of a tiling framework as describe by Ballier, Durand, Jeandel ([2], Section 2), let us divide the whole D-Cairo tiling into clockwise-mills (denoted further by C-mills), as shown in Figure (8, right, black contours). We will heavily employ this division in what is to follow. On the other hand, let us consider 24 different unit cells, 4 of which are shown in Figure 5 (to get them all, all possible permutations of 4 colors must be included). Simple considerations show that to properly color the D-Cairo board is the same task as to tile the plane with unit cells of 24 types ("states"), adhering to the following set of restrictions ("patterns"): for any state, there are 8 forbidden states to the N(orth), S(outh) (in the picture, 3 cannot be to the South of 1, but 4 can), E(east), and W(est), and 6 forbidden states to each of NE, NW, SE (4 cannot be to the SE of 1), and SW. Thus, we are in exactly the situation as described in [2]. Consequently, all structural results of authors apply.

Let us return to the fully colored D-Cairo board (we will use terms *full colouring of the tiling* and *full field* interchangeably). As a basic example, suppose a chain in two colors (**Blue** and **Yellow**) extends through the whole tiling (Figure 6 (a)). In such case

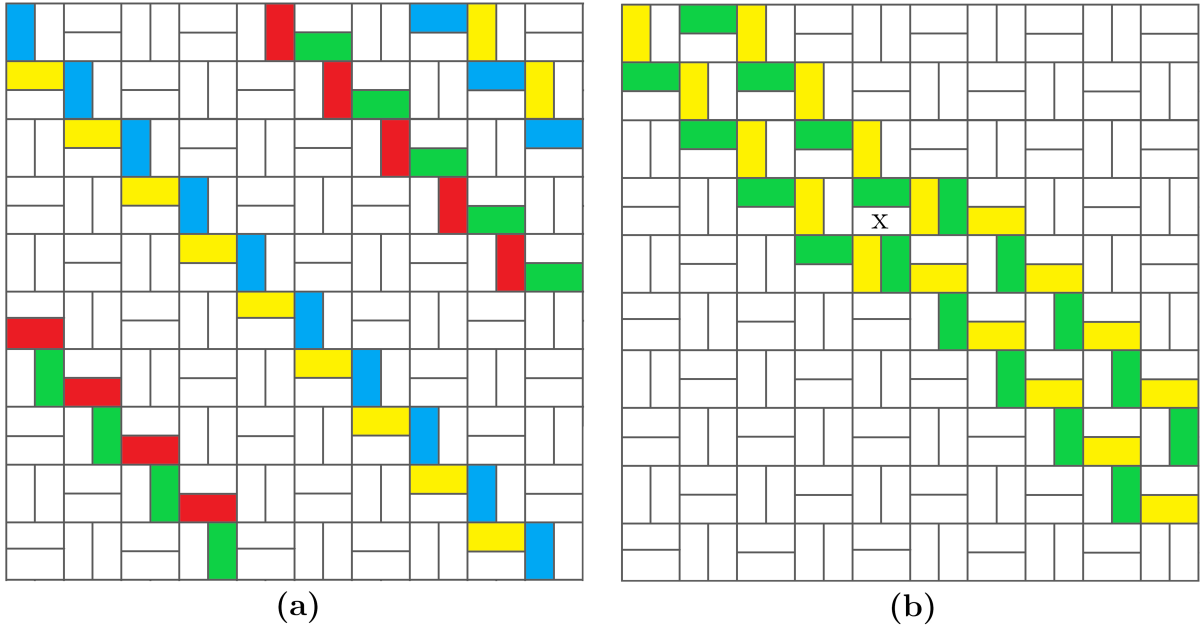


**Fig. 6** Type 1 wall (a) and Type 2 wall (b). A seed can be extended in the infinity (continuum) of ways if and only if their formation is not forbidden by the structure of the seed itself.

we call this chain *full type 1 wall*. A *simple wall* is its connected subset with at least 2 tiles (we will need this notion in Subsection 5). Another type 1 full wall must be built immediately below (and above) it to comply with the adjacency rule. For its coloring we have two choices: **R** and **G** in alternation, or the other way round. It is now obvious that each such coloring is in 1-to-1 correspondence with a doubly infinite sequence of 0's and 1's. As is well known, this has the power of continuum.

As a second basic example, in Section 5 we will witness that some finite patches generate *full type 2 wall* (same Figure (b), the lower T(op)L(ef)-B(ottom)R(ight) strip). Let us take a closer look at it. The tile x can be either **R** or **B**. In each case this forces coloring of strip of tiles, and we witness the formation of another type 2 wall of the exact the same pattern independently of our choice. In other words, the second type 2 wall immediately above is predestined, while a strip between them can be colored in two ways. The process continues. The number of degrees of freedom is halved, but it is still a countable set. Hence, all colorings have the power of continuum.

## 4 A perfect seed

It is all the more impressive that perfect seeds do exist!

Consider the seed in Figure 7 (a). A black point (the centre of coordinates) is for the orientation only.

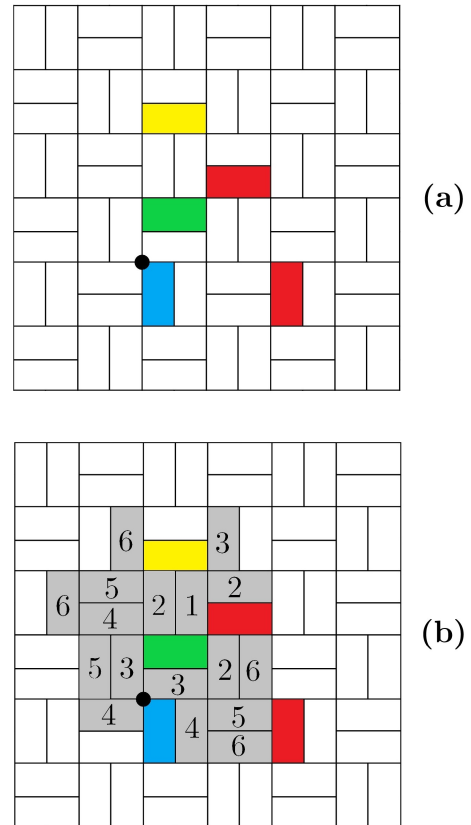


**Fig. 7** A perfect seed (a) and its stepwise growth (b)



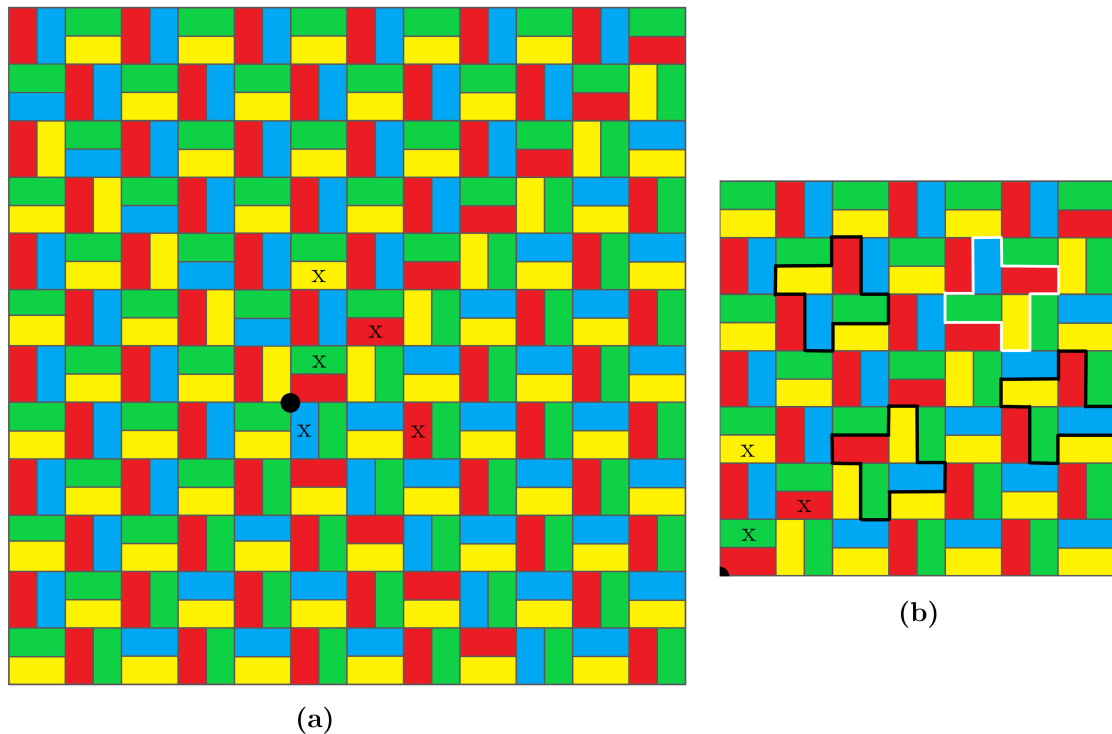


**Fig. 8** A central fragment of a perfect field (left) and its upper-right part

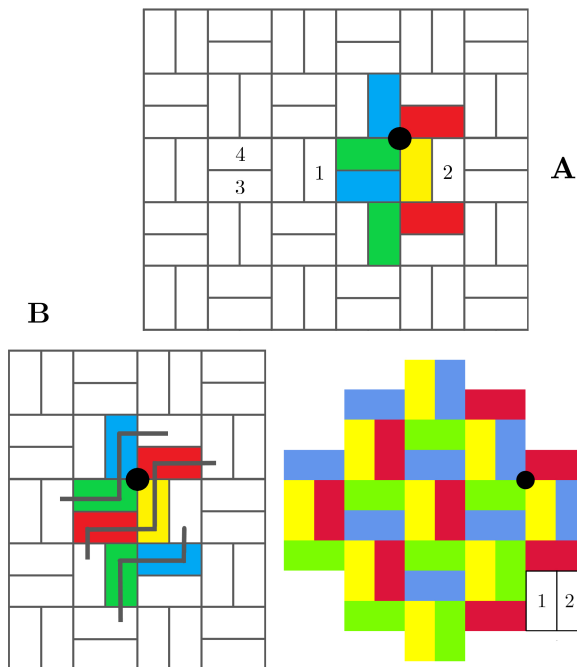


**Fig. 9** A configuration **A** always occurs in a full coloring without type 1 walls

Tile marked as 1 in (b) should be colored **B**, since it touches the remaining 3 colors. The first generation of newly colored tiles thus is a singleton. After that, we can color all the tiles labelled with

a number 2 (the second generation). Then with the number 3, and so on. Sometimes a new tile to be colored touches 4 tiles of preceding generations, but we never run into a contradiction, and the process continues. The number of tiles (say,  $t(n)$ ) we are able to color at step  $n$  gives the following sequence:

$$1, 3, 3, 3, 3, 4, 5, 5, 7, 7, 10, 12, 12, 14, 15, 18, 17, \dots$$

Its structure becomes apparent when we notice that  $t(n+1) - t(n)$  for  $n \geq 25$  periodically repeats the length 6 pattern  $(3, 0, 2, 1, 3, -1)$ . Thus for  $n \geq 25$ ,  $t(n) = \lfloor \frac{4n}{3} \rfloor - 3 + c(n)$ , where  $c(n)$  periodically repeats  $(-1, 1, -1, 0, 0, 1)$ . We also notice that the tiles from a fixed generation form a circular-like domain, and every tile of the plane will eventually be colored.

The final result is shown in Figure 8 (a). The field produced by the seed seems rather periodic, but at certain  $1 \times 1$  cells the pattern breaks. As already mentioned, let us divide a whole field into C-mills, as shown in Figure 8 (b) by black contours (for a moment, ignore the white anti-clockwise windmill, denoted further by A-mill).

It appears that there are only 5 different types (“states”) of mills. If we replace each combination with a single color, we arrive to Figure 10 (top left). What a surprise! Each colored component is a part of a periodic  $2D$  or  $1D$  structure (“a crystal”). If we

used A-mills instead, the picture would have been the one shown on the right, with 6 distinct colors needed.

This is clearly a poly-crystallite material produced by a local assembly rules. The last question we need to answer is the following: does its structure depend on our choice? In other words, if we divide the field into fundamental domains of 4 tiles each in a different fashion (white A-mills as shown in Figure 8 (b), or into squares  $2 \times 2$ ), and define a coloring scheme, will the final result will be visually any different?

The answer is “No”. The division is certainly up to us. However, human cognitive system is very good in noticing regularities in visual micro-patters. Essence of this phenomenon is described by psychological *Gestalt laws of grouping*. So, let us color 100 generations of the seed (MAPLE does this job for us). The result is shown in Figure 11. Our eyes clearly witness the structure of the material. In particular, we see that the boundary between 1 and 2 is more eminent than the one between  $1'$  and  $2'$ . This is confirmed by Figure 10 (top left and right). Indeed,  $1'$  and  $2'$  are immediately adjoined, while 1 and 2 are separated by a  $1D$  defect.

## 5 All polycrystals

At this point, many natural question arise. First: are there any other essentially distinct examples? For the starters, we note that the symmetry group of D-Cairo tiling (denoted in crystallography by  $p4g$ ) includes the reflection with respect to the line  $x = \frac{1}{2}$ . However, when we collect all 4 dominoes around every vertex  $(x, y) \in \mathbb{Z}^2$ ,  $x + y \pmod{2} = 1$  (“odd vertices”, as opposed to “even” ones) into C-mills, the reflection symmetry is lost: such transformation carries a C-mill into an A-mill. However, this particular grouping is our subjective choice, it is not present in a tiling itself. This remark has the following consequence: when we classify all perfect fields, both versions of mills must be considered. With that said, we can state our first main result.

**Theorem 1** *Suppose a finite 4-color seed in the D-Cairo tiling forces the full coloring. Then, up to the symmetry of the tiling and permutation of colors, the full field is one of two kinds:  $\mathfrak{Y}$  or  $\mathfrak{X}$  (shown in Figure 10).*

To prove this, suppose we have such a seed. Let us color the whole field. Clearly, at every vertex (even or odd) where 4 tiles meet, all 4 colors are present. We will choose such a vertex as a starting point having the following additional criteria in

mind.

As we have seen in Section 3, such a coloring cannot contain a full type 1 wall. Choose any even vertex. Let BL and BR colors be  $\mathbf{G}$  and  $\mathbf{Y}$  (Figure 9 **A** and **B**). These two tiles already form a simple wall, oriented as TL-BR. We go along this wall in the direction where it terminates. It does when a third color occurs. A simple reasoning shows that a configuration can be either **A** or **B** (Figure 9). However, in the latter case we see a formation of three parallel simple type 1 walls, this time oriented as BL-TR. Going along these in the direction where one of them terminates convinces us that we are back to the setting **A**. So, without loss of generality, we can take the latter as a starting point.

Choose 4 cells (marked 1, 2, 3, 4 in the figure) so that there is no conflict with the adjacency rule. For example, we can take colors  $(\mathbf{Y}, \mathbf{G}, \mathbf{B}, \mathbf{G})$ . In total, there are  $2 \times 2 \times 4 \times 3 = 48$  possibilities. MAPLE code works on such input. If eventually a cell neighbouring 4 distinct colors is encountered, the program halts with a FAULT. If the program can run on infinitely, it produces a pre-given number of generations.

Here is the outcome. The program halts in 38 cases. In 7 cases we witness the growth of a polycrystal very similar to the one described in Section 4. However, a closer look reveals some differences. In order to understand the situation better, an extension of the program was added. The latter automatically subdivides the board into C-mills (and, independently, A-mills) and re-colors it. In general, 24 colors are needed. However, if we accept the metaphor of a “mill”, we may consider cyclic permutations of colors as being close variants of one another. This suggests the following scheme. 6 colors groups, each consisting of 4 hues, are chosen: yellow-gold, green-olive, grey-silver, red-pink, cyan-turquoise, blue-violet. Permutations of 4 colors belong to the same group if they are cyclic. This convention applies to C-mills. For A-mills, we imagine it reflected with respect to the vertical line. Now it is C-mill and it has its own color.

The rest is done by the program. The choice  $(1, 2, 3, 4) = (\mathbf{Y}, \mathbf{G}, \mathbf{Y}, \mathbf{G})$  leads to the picture shown in Figure 10 (middle). Analogous picture (in case of necessity we switch C-mill with A-mill) occurs in 4 more cases. We label the A-mill configuration as  $\mathfrak{Y}$ . On the other hand, the choice  $(1, 2, 3, 4) = (\mathbf{Y}, \mathbf{G}, \mathbf{B}, \mathbf{Y})$  leads to the picture shown at the bottom. This occurs in one more case. We label the C-mill version as  $\mathfrak{X}$ . Its pleasingly symmetric, and the whole polycrystal consists of one

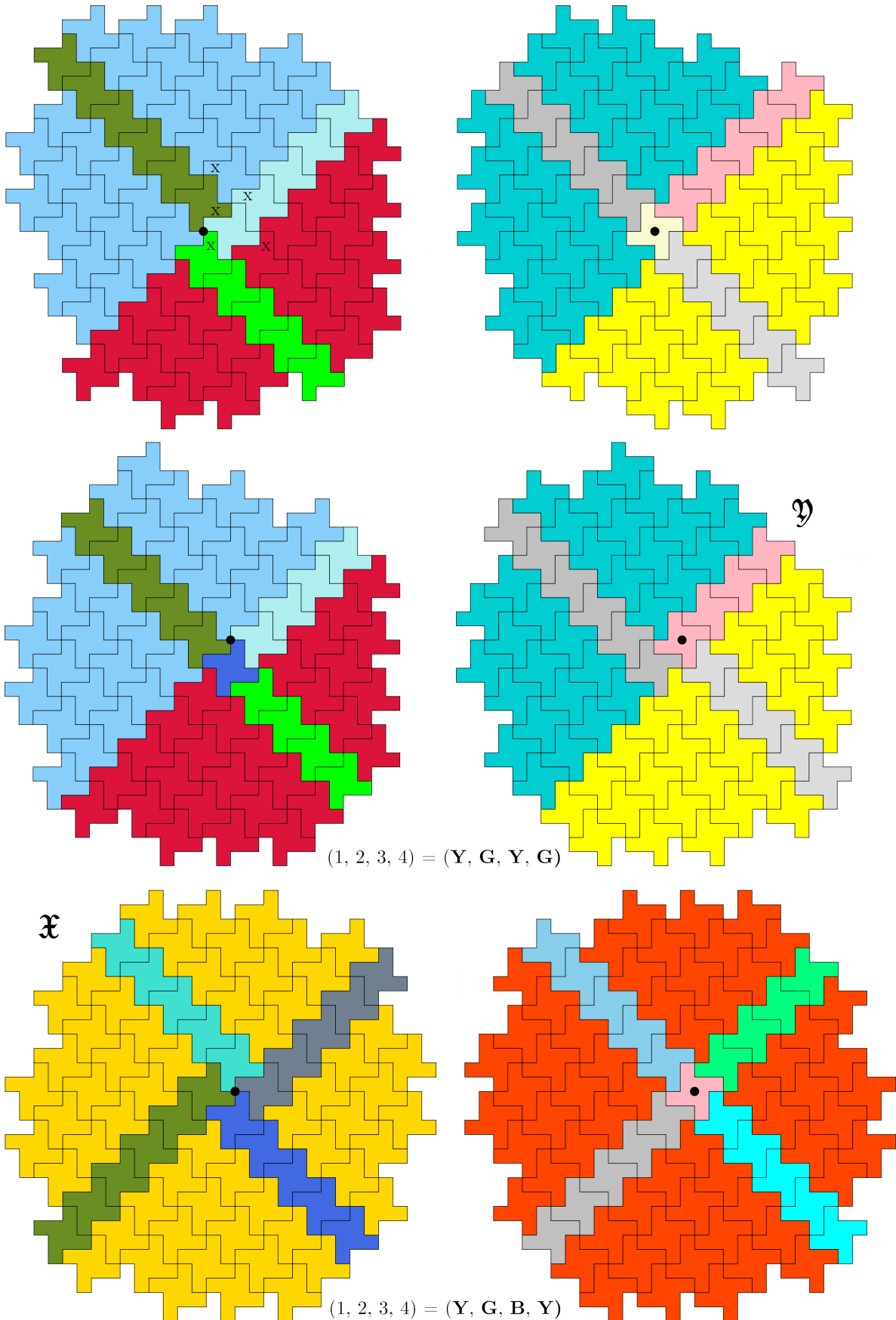
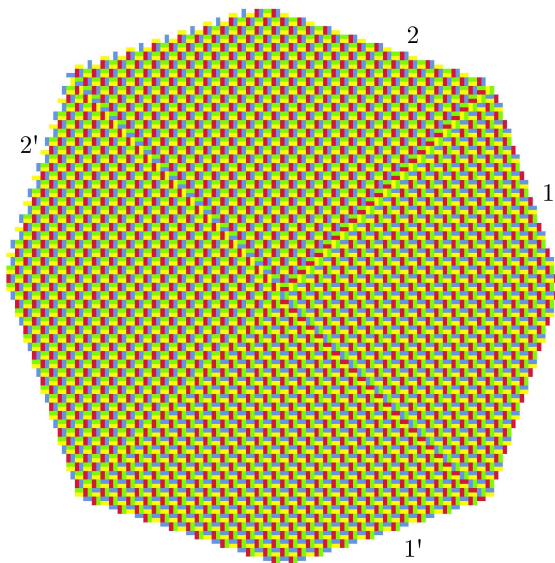


Fig. 10 Fields of perfect seeds divided into windmills



**Fig. 11** 100 generations, produced by the perfect seed

single crystal with four 1D defects. Its A-mill version shows that a central “molecule” (light pink) is a rotation of main (orange red) molecule.

Next, out of 48 cases, two lead to the formation of full type 2 wall (Figure 6, left) and so must be discarded.

We are left to consider the final choice  $(1, 2, 3, 4) = (\mathbf{R}, \mathbf{B}, \mathbf{B}, \mathbf{G})$ . In this case the program does not halt, but it colors only the tiles shown in (Figure 9, bottom right). Now, all possible choices of tiles 1 and 2 lead either to type 2 wall or a contradiction. This completes the proof of the theorem.

## 6 Decent seeds and defects

Having dealt with perfect fields, we have all the tools needed to prove the second main result.

**Theorem 2** *The cardinality of extensions of any given seed is either finite or a continuum.*

*The 2-tile seed shown in Figure 12 (a) is decent and is of order 36. There exist decent seeds of orders 1, 2, 3, 4, 6, 12.*

Let  $P$  be a finite patch. Confine it to the square  $\mathcal{S} = [-N, N] \times [-N, N]$ , where  $N \in \mathbb{N}$  is a sufficiently large. Suppose,  $P$  cannot be extended in a continuum of ways. This implies that  $P$  is not part of a coloring consisting only of TL-BR or BL-TR full type 1 system of walls. Now, for any full coloring, tiles inside  $\mathcal{S}$  have their own color. Consequently, we can run over all colorings of  $\mathcal{S}$  which extend  $P$

and comply to the adjacency rule, to check whether it has a further extension to the full field. Due to convention about non-continuum, a configuration  $\mathbf{A}$  (Figure 9) is always to be found inside  $\mathcal{S}$ . Since type 2 walls are also excluded, the number of extensions must be finite.

From a computation point of view, it is easy to check whether a given patch belongs to a system of type 1 or type 2 walls. Counting the order of a decent seed can also be accomplished in a polynomial time. Truly, let us confine a seed to a square  $\mathcal{S}$  again. Choose an odd vertex  $\mathbf{p} \in \mathcal{S}$ . Let us place all  $4 \times 24$  possible polycrystals with  $\mathbf{p}$  as its center. It is enough to check whether a particular polycrystal extends the seed. To implement this in reality is another matter. It is completely unclear which integers can occur as orders of decent seeds. The second half of the Theorem gives the partial answer, whereas the full solution requires a separate research.

And so, consider two red tiles given in Figure 12 (a). They are located in such a mutual position which (as the reader can check) eliminates the possibilities of type 1 or type 2 walls. To prove the property stated, consider windmills at  $(1, 1)$ , afterwards at  $(1, 2)$ ,  $(2, 2)$ . We see that tiles 1 and (afterwards) 2, 3 are forced to be  $\mathbf{R}$ .<sup>3</sup> Next, running the program through all admissible variants of a mill at  $(0, 0)$ <sup>4</sup> we get that 4 is also forced to be  $\mathbf{R}$ , and so do afterwards 5, 6. Further, tile 8 is not  $\mathbf{R}$ . If a tile 7 were not  $\mathbf{R}$ , then 9 and 10 would have the same (not  $\mathbf{R}$ ) color, and so would 11 and 12 – a contradiction. Thus, 7 is also  $\mathbf{R}$ .

At this point, if an extensions exists, three remaining colors can be arbitrarily permuted. Suppose  $(13, 14) = (\mathbf{G}, \mathbf{Y})$  (Figure 12 (b), the numbering is now reset). Running the program through all possible choices of tiles 1, 2, 3, 4, we obtain 6 collections leading to perfect seeds (Figure 13). The rest choices give a FAULT. Finally, we can fix several out of 6 variable (non- $\mathbf{R}$ ) tiles in Figure 13 to obtain decent tiles of all orders listed. Theorem is proved.

Here is another direction of research where one can go. It is inspired by Figure 7 in [11], a decapod defect in the Penrose tiling which forces the full coloring. Concerning a D-Cairo board, let us say that its coloring has *defects*, if an adjacency rule is breached at a finite number of vertices or edges. Since there are many combinatorial configurations of possible

<sup>3</sup>Just two red tiles force a countable number of  $\mathbf{R}$ eds: North of A-mills at  $(n - 1, n)$ , and East of C-mills at  $(n, n)$ ,  $n \in \mathbb{N}$ .

<sup>4</sup>We need to check only two cases, which can be done by hand. Indeed, permutation of colors  $\mathbf{Y}, \mathbf{B}, \mathbf{G}$  does not impact on where program halts with a FAULT.

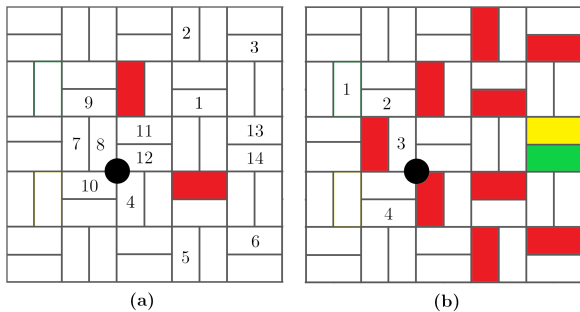


**Fig. 12** A decent seed (a), and one of 6 its possible extensions (b)

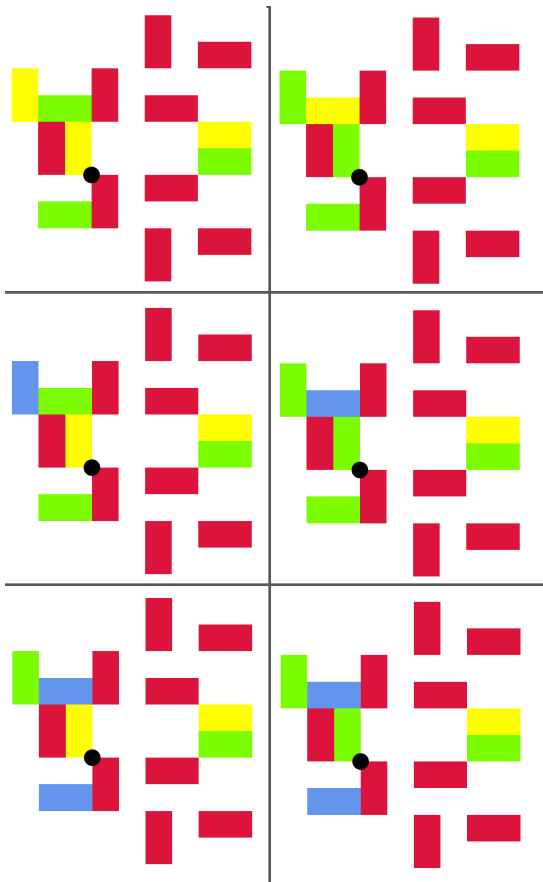


**Fig. 13** Perfect seeds, possible extensions a decent seed in Figure 12 (b). Permutations of  $\mathbf{G}, \mathbf{Y}, \mathbf{B}$  give 36 extensions of the seed in Figure 12 (a).

defects, let us confine to the simplest case: all possible defects are at the centres of A-mills (either both tiles N&S, or both E&W have the same color). Figure 14 shows an example of a polycrystal with one such defect. What happens if two defects are allowed? What is the number  $\mathcal{T}$  (if finite) of different polycrystals? In general,  $\mathcal{T}$  depends on coordinates of one defect with respect to the other. Thus we define an integer function  $\mathcal{T}(m, n)$ . If  $\mathcal{T}(m, n) < \infty$ , what is the exact value?

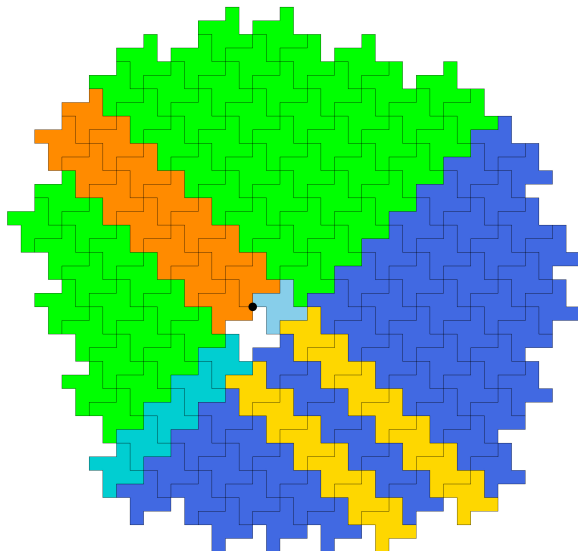


**Fig. 14** Polycrystal with one defect (shown in white)

## 7 A toy model

Let us consider our tiles as 24 versions of squares (see Figure 5 again). We will show that the matching rules can be realised by euclido-geometric restrictions.

For this purpose consider a  $2 \times 2 \times 2$  cube (“a molecule”). It consists of 8 “atoms”, two copies of each of  $\mathbf{R}, \mathbf{G}, \mathbf{B}, \mathbf{Y}$ , identical atoms being placed on opposite ends of long diagonals. All molecules thus only differ in their spacial orientation. Inside the  $xy$  plane, consider the lattice  $\mathbb{Z}^2$  and its index 10 sublattice  $\mathcal{L} = (-1, 3)\mathbb{Z} \times (3, 1)\mathbb{Z}$ . For each  $\mathbf{p} \in \mathcal{L}$ , let us place a molecule with  $\mathbf{p}$  as its centre, so that the upper face of a molecule is parallel to the  $xy$  plane, and its edges are aligned with the axes  $x, y$ . Figure 15 shows 4 examples. The process now runs as follows: at every discrete tick of a time, one molecule makes several  $\pm 90^\circ$  rotations around its centre with respect to any of the axes  $x, y$ , and  $z$  (in the picture, the latter is directed towards the viewer). This is called *an orientation change*. The adjacency rule translates into the language of molecules as follows:

**AR:** *the distance between atoms of the same kind must be greater than 2.*

Note that for each atom there are exactly 7 other atoms at a distance  $\leq 2$ . For example, if we choose  $\mathbf{G}$  as shown in Figure 15, 6 of these close neighbours belong to the plane  $z = 1$ , while the remaining one, namely,  $\mathbf{Y}$ , lies on the plane  $z = -1$  immediately below  $\mathbf{G}$ . The former is paired with  $\mathbf{Y}$  shown on the picture. During the process, each molecule strives to attain orientation which is compliant with the **AR**. According to R. Penrose, Euclidean geometry is the first SUPERB physical theory ([5]). Thus, the

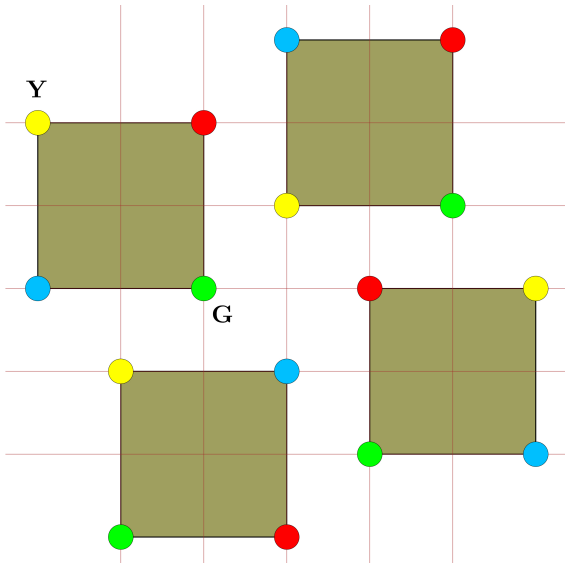


**Fig. 15** 4 molecules corresponding to 4 central windmills in Figure 10 (top left)

above construction gives a neat “physical model” of our coloring problem, translating matching rules into a single geometric restriction. Possibly, this toy is implementable relying solely on mechanics (like an analogue of Rubik’s cube for each molecule) and magnetism (a pair of magnets for each color). Six faces of a cube can be given 6 colours and certain textures, which, if rotated, would reflect a slightly different hue. This would be in correspondence with coloring scheme used in two previous sections.

## 8 Type 7 pentagonal tiling

To show that the D-Cairo tiling is not an isolated phenomenon where forced grain boundary occurs, consider 2-isohedral pentagonal tiling of type 7 (discovered by R. Kershner, Figure 16). Its extreme case is topologically equivalent quadrilateral tiling (denoted in this section by K, see Figure 17).<sup>5</sup>

Perfect seeds do exist for the tiling K, too. One of them is shown in Figure 17. The fundamental domain (shown in Figure 19 as a brown contour) consists of 8 tiles. There appears to be 144 types of colorings of 8 tiles, which comply to the adjacency rule. One can invent a new coloring scheme with 144 colors in the palette and present the pictures.

But none of that is needed. In fact, it is possible to work with the same D-Cairo tiling. To demonstrate that this, let us map all tiles 1-8 in the fundamental domain of a K-tiling to the properly

chosen 8 tiles in D-Cairo tiling, as shown in Figure 19. Thus, the same D-Cairo geometry is being used, only the set of 7 neighbours for each tile of the field is re-defined.

Now, if we calculate 80 generations of the perfect seed in Picture 17 and transport the picture to the D-Cairo field via a map given, we obtain Figure 18.

One clearly sees a grain boundary emerging. What is unexpected is that the growth of the polycrystal in the right direction is faster than in the left. Let us take a final look to the map in Figure 19. Tiles 2, 4, 6, 8 from one fundamental domain mutually touch one another. We can color the corresponding C-mill in the D-Cairo field according to our previous coloring convention. The same applies to tiles 1,3, 5’, 7”, this time tiles 5’ and 7” come from two neighbouring fundamental domains. The picture obtained is shown in Figure 20.

In order to finally convince oneself that this grain boundary is of a different kind than those described in Section 5, let us start again from the seed in Figure 17 and count the number (say,  $k(n)$ ) of tiles we are able to color at step  $n$ . This produces the sequence

1, 3, 3, 3, 2, 2, 4, 3, 4, 6, 8, 9, 11, 12, 14, 12, 16, 16, ...

It appears that  $k(n + 1) - k(n)$  is also eventually periodic. Here is the final result: for  $n \geq 37$ ,  $k(n) = \lfloor \frac{15n}{14} \rfloor + c(n)$ , where  $c(n)$  is a sequence with period 336. Proving exact values for coordination sequences even for the basic tilings is not a simple task (see [9]). Thus, to rigorously prove the results stated about the sequences  $t(n)$  and  $k(n)$  might be much harder than to check this experimentally.

Going over many other examples given, say, in the masterpiece of the field [7], will hopefully produce even more grain boundaries.

*Acknowledgement.* The author sincerely thanks the anonymous referee whose benevolence helped greatly in placing the results of this paper into a much broader context of aperiodic tilings.

## References

- [1] XIE ZHANG et al, First-principles calculations of defects and electron-phonon interactions: Seminal contributions of Audrius Alkauskas to the understanding of recombination processes, *J. Appl. Phys.* **135** 150901 (2024), <https://pubs.aip.org/aip/jap/article/135/15/150901/3283072/> [First-principles-calculations-of-defects-and](https://pubs.aip.org/aip/jap/article/135/15/150901/3283072/First-principles-calculations-of-defects-and)

<sup>5</sup>One can play around all 15 known types of pentagonal tilings on a Wolfram tool [14].



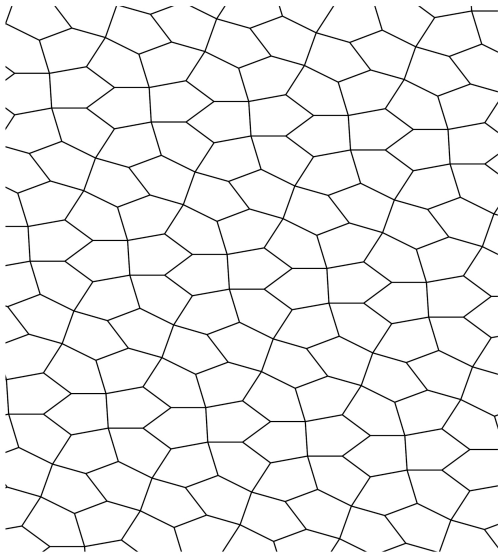


Fig. 16 Pentagonal type 7 tiling

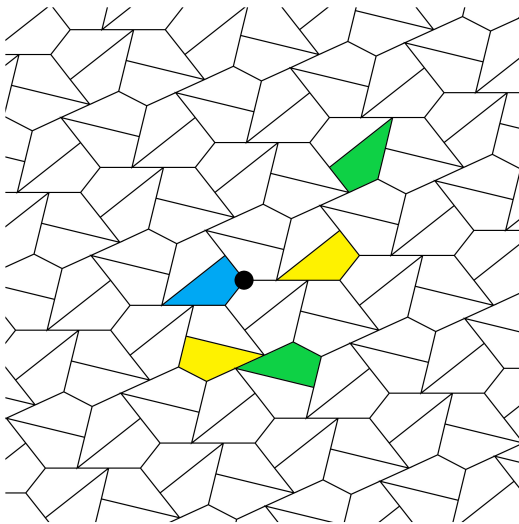


Fig. 17 A perfect seed

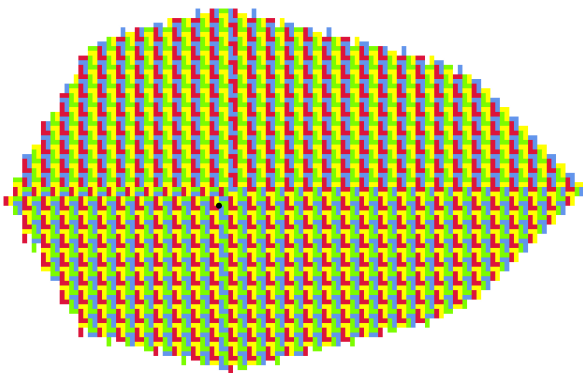


Fig. 18 80 generations of the see in Figure 17

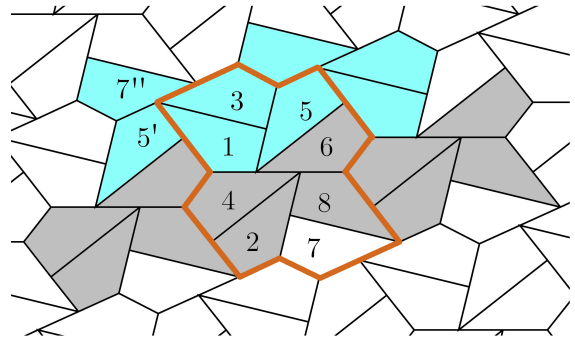
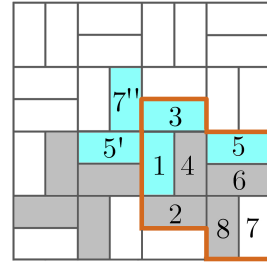


Fig. 19 The map from type 7 pentagonal to the D-Cairo

- [2] A. BALLIER, B. DURAND, E. JEANDEL, Structural aspects of tilings. *STACS 2008: 25th International Symposium on Theoretical Aspects of Computer Science*, (2008), 61–72, <https://hal.science/hal-00145800v1/file/questions.pdf>
- [3] CONNOR T. HANN, J. E. S. SOCOLAR, P. J. STEINHARDT, Local growth of icosahedral quasicrystalline tilings, *Phys. Rev. B* **94**, 014113 (2016), <https://doi.org/10.1103/PhysRevB.94.014113>.
- [4] S. DWORKIN, J.-I. SHIEH, Deceptions in quasicrystal growth, *Comm. Math. Phys.* **168**(2), (1995) 337–352, <https://link.springer.com/article/10.1007/BF02101553>
- [5] R. PENROSE. *The emperor's new mind. Concerning computers, minds, and the laws of physics*. With a foreword by Martin Gardner. The Clarendon Press, Oxford University Press, New York, 1989.
- [6] CHARLES RADIN, Conway and aperiodic tilings. *Math. Intelligencer* **43** (2)(2021), 15–20, <https://link.springer.com/article/10.1007/s00283-020-10038-6>
- [7] B. GRÜNBAUM, G. C. SHEPHARD, *Tilings and patterns*, Freeman and Company, New York, 1987.

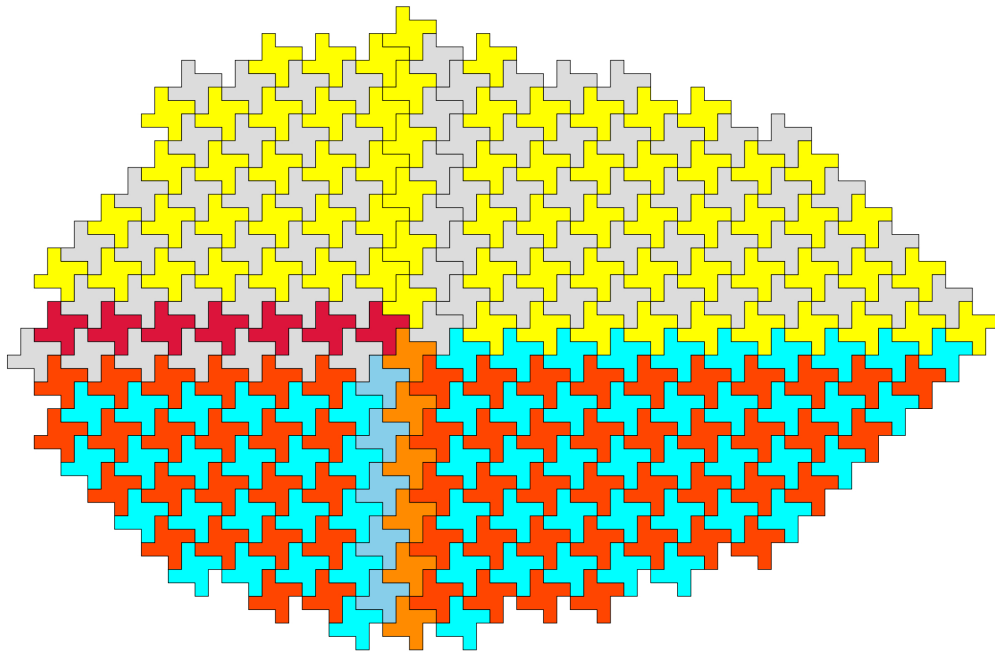


Fig. 20 “Even” and “odd” part of the same field

- [8] CH. GOODMAN-STRAUSS Can’t Decide? Undecide!, *Notices Amer. Math. Soc.*, **57** (3) (2010), 343–356, <https://www.ams.org/notices/201003/rtx100300343p.pdf> [pii/S0097316511000859](https://doi.org/10.1090/S0097316511000859)
- [9] C. GOODMAN-STRAUSS, N. J. A. SLOANE, A coloring-book approach to finding coordination sequences. *Acta Crystallogr. Sect. A* **75**(1) (2019), 121–134, <https://doi.org/10.1107/S2053273318014481>
- [10] D. SMITH, J. S. MYERS, C. S. KAPLAN, C. GOODMAN-STRAUSS, An aperiodic monotile, *Combinatorial theory*, **4**(1) (2024), #6 <https://doi.org/10.5070/C64163843>.
- [11] J. E. S. SOCOLAR, Growth rules for quasicrystals. *Quasicrystals*, 225–250, Dir. Condensed Matter Phys., 213–238. World Scientific Publishing Co., 1991, [https://doi.org/10.1142/9789814503532\\_0008](https://doi.org/10.1142/9789814503532_0008)
- [12] J. E. S. SOCOLAR, J. M. TAYLOR, Forcing Nonperiodicity with a Single Tile, *Mathematical Intelligencer* **34** (1), 18–28, (2012), <https://link.springer.com/article/10.1007/s00283-011-9255-y>
- [13] J. E. S. SOCOLAR, J. M. TAYLOR, An aperiodic hexagonal tile, *Journal of Combinatorial Theory, Series A* **118** (8) (2011), 2207–2231, <https://www.sciencedirect.com/science/article/>
- [14] ED PEGG JR, *Pentagon tilings*, Wolfram Demonstrations Project <https://demonstrations.wolfram.com/PentagonTilings>.